European Rotorcraft Forum

ENHANCED GUST LOAD RECOVERY FOR THE AW609 TILTROTOR

Federico Fonte, federico.fonte@leonardocompany.com, Leonardo S.p.A. Helicopter Division (Italia)
Marco Favale, marco.favale@leonardocompany.com, Leonardo S.p.A. Helicopter Division (Italia)
Alberto Rigo, alberto.rigo@polimi.it, Politecnico Di Milano (Italia)
Giuseppe Quaranta, giuseppe.quaranta@polimi.it Politecnico Di Milano (Italia)

Abstract
The prediction of dynamic gust loads for a tiltrotor is a challenging task since it requires to take in account several components such as the flexibility of the airframe and of the rotor, their aerodynamic properties and the effect of the automated flight control systems. The characterization of the aerodynamic forces acting on the tiltrotor, in particular, can be very difficult and the direct use of unsteady aerodynamic forces from simplified panel methods can lead to a wrong definition of the dynamic properties of the rigid modes of the aircraft. A correction of the unsteady aerodynamic forces using tabulated stability derivatives can then be used to recover the proper aircraft dynamics. The use of a reduced basis for the characterization of the structural dynamics can lead to a poor accuracy of the predicted loads, and the mode acceleration method can be used to solve this problem. The present paper describes the advantages obtained using the mode acceleration method for load recovery and presents a procedure for the correction of aerodynamic forces using tabulated aerodynamic coefficients, showing their effect on the gust loads.

1. INTRODUCTION

A lot of effort is being devoted at Leonardo Helicopters to develop technologies able to model the aeroelastic response of complex configurations, such as tiltrotors where the rotor dynamics, the flexibility of the aircraft and the flight control system play all together a significant role. Dynamic gust response analyses are required by regulations for the evaluation of airframe loads. The results of these analyses are strongly affected by the accurate modeling of the coupling among all the aircraft components. In the evaluation of gust loads it is important to reproduce accurately the low-frequency response of the whole aircraft and at the same time to model the aircraft flexibility and the unsteady aerodynamic effects. In addition to the response of the aircraft it is also important to accurately reproduce the load distribution on the structure. This is particularly true for tiltrotors for which some early studies[1,2] showed how the loads response to lateral and longitudinal gusts in high-speed airplane mode flight is higher than that of conventional turboprop, thus requiring an accurate representation of rotor dynamics and its coupling with the airframe. The main differences are related to the presence of large nacelle-rotor masses at wing tip that lead to low-frequency structural modes, and the flexibility of proprotors that exert a significant influence on the developed unsteady loads. The additional presence of a fly-by-wire control system creates further complexity, since it influence on the aircraft dynamics and loads can be quite substantial, see[3].

To simulate the dynamic response of these complex configurations a Matlab-based tool has been developed by Politecnico di Milano and Leonardo Helicopters[4,5] and has already been applied to the evaluation of the gust dynamic response of tiltrotors[6,7,8]. However, some improvements to the methodology were deemed necessary, concerning in particular the accuracy in the reproduction of the flight dynamics modes of the aircraft and the possibility to recover internal forces in the structure in a more accurate yet simple way.

An extensive database of aerodynamic coefficients for the rigid aircraft is usually available for the use in flight mechanics stability analyses, for Flight Control System (FCS) design and for the development of flight simulators. This database can originate from a combination of wind tunnel experimental data, high-fidelity aerodynamic analyses and flight tests and allows an accurate reproduction of the low-frequency dynamic response of the aircraft. The objective here is to introduce this data in

aeroelastic simulations allowing for a more accurate definition of the short period and dutch roll modes, that in turn can greatly affect the dynamic gust response and the related structural loads.

The superimposition of modes is a well established methodology for the evaluation of the dynamic response of a structure. In fact, the direct response approach becomes soon impractical, or even impossible, when the degrees of freedom of the model grow. Moreover, the alternative approach implemented in NASTRAN and other Finite Element Software, of direct summation of external forces, included inertial and aerodynamic ones, cannot be applied on complex structure with multiple load path[6].

In the standard approach, denominated mode truncation, starting form an analysis of the bandwidth of the excitation input to the aircraft, it is possible to select the range of structural modes that will be dynamically excited in the the system and, used them for dynamic simulation and load recovery, neglecting the contribution of all other modes[9]. Unfortunately, to bring the truncation error on internal loads to an acceptable level, as shown in Ref. [6], it is necessary to extend the range of selected modes much more than what a simple dynamic response would require. Additionally, in many cases it is not possible to obtain a monotonic converging behavior of the error.

The other approach, denominated Mode Acceleration, and developed principally in the aerospace field[10], stems from a very simple consideration: all truncated modes are outside the frequency range of interest of the input. Consequently, they will respond statically and so their response will affect loads but it will not affect significantly the dynamic response that can be computed without keeping them into account[9]. While the idea of mode acceleration is very simple the application of this approach to a multidisciplinary model, composed by many sub-blocks developed through state-of-the-art software and then connected, may be particularly cumbersome. The paper will present the steps required to achieve the capability to perform mode acceleration within the MASST suite. It will show how the better convergence given by the use of the mode acceleration method allows for the use of more efficient dynamic models and it also simplifies the generation of the state-space model that is required to represent the unsteady aerodynamic forces in time domain.

The aim of this paper is to present the methodology used for the correction of aerodynamic coefficients and the implementation of the mode acceleration method. The application of this methodology to the dynamic gust response analysis for the AW609 aircraft is also presented, along with the comparison of the results with respect to those obtained with the baseline method.

2. TILTROTOR MODEL

The generation of the aeroservoelastic model of the AW609 tiltrotor requires the availability of different numerical models for its components (airframe, rotors, FCS etc.) that are first generated using specific software and then integrated in a single aeroelastic model by the MASST suite. A Nastran Finite Element Model (FEM) is used to reproduce the structural dynamics of the airframe, coupled with unsteady aerodynamic forces computed using the Doublet Lattice Method (DLM). The airframe model is then connected to the linearized structural and aerodynamic model of the rotors, the dynamic model of the control surface actuators that includes their compliance, the model of the Flight Control System (FCS) and the related sensors, leading to the full model presented in Fig. 1.

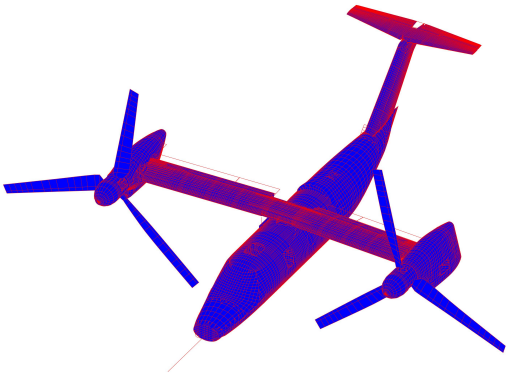

Figure 1: MASST model of the AW609 tiltrotor.

The model is based on an accurate FEM of the fuselage, wing, nacelles and tail, implemented in NASTRAN and out of which the structural modal frequencies and shapes are computed[11]. Two CAMRAD II[12] elastic rotor models are connected to the airframe. A database of linearized models associated with several trim conditions is generated within the flight envelope. This database includes the gimbal degrees of freedom of the rotor and several elastic blade degrees of freedom, together wit the possibility to apply collective and cyclic controls, as required by the Flight Control System. Linear servoactuator

transfer functions have been defined for the collective and cyclic actuators of the rotor swashplates and for the actuators of the aerodynamic control surfaces (the two flaperons and the elevator). A detailed Doublet Lattice Method (DLM) model, developed in NASTRAN, is added to compute unsteady loads developed by the aiframe, including the effect of movable surfaces[13].

Unsteady aerodynamic forces associated to small motion of the airframe and gusts can be obtained as solutions of integro-differential equations related to harmonic boundary domain oscillation[13] suing the DLM approach. In this case all loads are computed in the frequency domain as,

$$\boldsymbol{f} = \boldsymbol{f}_a + \boldsymbol{f}_g = q_\infty \boldsymbol{H}_{am}(k,M)\boldsymbol{q} + q_\infty \boldsymbol{H}_{ag}(k,M)\frac{\boldsymbol{U}}{V} \tag{1}$$

where q_∞ is the dynamic pressure, $k = \frac{\omega c}{2V}$ is the reduced frequency obtained by using the half-chord $c/2$ as reference length, M is the Mach number, $\boldsymbol{H}_{am}$ and $\boldsymbol{H}_{ag}$ are the aerodynamic transfer matrices associated to the structural mode shapes $\boldsymbol{q}$ and to the gust input speed $\boldsymbol{U}$[11]. MASST can cast the resulting frequency domain matrices in state-space form, using the approach described in[14,15]:

$$\begin{aligned} \boldsymbol{x}_a' &= \boldsymbol{A}\boldsymbol{x}_a + \boldsymbol{B}\boldsymbol{a} \\ \boldsymbol{f}/q_\infty &= \boldsymbol{C}\boldsymbol{x}_a + \boldsymbol{D}_0\boldsymbol{a}' + \boldsymbol{D}_1\boldsymbol{a}' + \boldsymbol{D}_2\boldsymbol{a}'', \end{aligned} \tag{2}$$

where $\boldsymbol{a} = \{\boldsymbol{q};\boldsymbol{U}\}$ and the apex ($'$) represents a derivation with respect the non-dimensional time $\tau = \frac{t2V_\infty}{c}$. . The transformation of the frequency domain gust terms for unsteady loads into a time domain formulation requires some care, as shown in[16,6].

This transformation is essential, because it allows to perform within MASST time domain simulation of gust and maneuver response, using linear and nonlinear time domain models of the FCS.

3. AERODYNAMIC MODEL CORRECTIONS

The linear lifting surface method used to compute unsteady aerodynamic forces is not able to accurately predict the interference between wing and fuselage and nacelles, as well as the effect of airfoil thickness and curvature. In particular the aerodynamic coefficients affecting the flight mechanics of the aircraft are often poorly predicted leading to an inaccurate evaluation of flight mechanics modes. In particular the short period and dutch roll frequencies and damping ratios can be inaccurate, affecting significantly the gust response. Consequently, it is important to correct the aerodynamic matrices introducing a more accurate prediction of the aircraft aerodynamic coefficients. Aerodynamic coefficients can be obtained from experimental data or high-fidelity computational methods, and usually are expressed in form of derivatives with respect to the body velocities:

$$\boldsymbol{f}_a = \boldsymbol{C}^{DB}_{body}\boldsymbol{v}_b = \boldsymbol{C}^{DB}_{body}\begin{bmatrix} \bar{u} \\ \beta \\ \alpha \\ \bar{p} \\ \bar{q} \\ \bar{r} \end{bmatrix} \tag{3}$$

where $\boldsymbol{C}^{DB}_{body}$ is built using aerodynamic coefficients extracted from an available database. Since only linear perturbations around an equilibrium configuration are considered here, it is possible to find a linear relationship between the body velocities in $\boldsymbol{v}_b$ and the model degrees of freedom associated to its rigid motion in an inertial reference frame $\boldsymbol{x}_i = [u_x, u_y, u_z, \theta_x, \theta_y.\theta_z]^T$, that are typically used for aeroelastic models. The general transformation depends on the reference flight condition used for the linearization[17] and for the special case of level flight it simplifies to

$$\boldsymbol{v}_b = \boldsymbol{T}_1\boldsymbol{x}_i' + \boldsymbol{T}_0\boldsymbol{x}_i \tag{4}$$

where

$$\begin{aligned} \boldsymbol{T}_1 &= \frac{2}{c}\begin{bmatrix} 1 & 0 & 0 & 0 & 0 & 0 \\ 0 & 1 & 0 & 0 & 0 & 0 \\ 0 & 0 & -1 & 0 & 0 & 0 \\ 0 & 0 & 0 & b/2 & 0 & 0 \\ 0 & 0 & 0 & 0 & c/2 & 0 \\ 0 & 0 & 0 & 0 & 0 & b/2 \end{bmatrix}; \\ \boldsymbol{T}_0 &= V_\infty \begin{bmatrix} 0 & 0 & 0 & 0 & 0 & 0 \\ 0 & 0 & 0 & 0 & 0 & 1 \\ 0 & 0 & 0 & 0 & 1 & 0 \\ 0 & 0 & 0 & 0 & 0 & 0 \\ 0 & 0 & 0 & 0 & 0 & 0 \\ 0 & 0 & 0 & 0 & 0 & 0 \end{bmatrix}; \end{aligned} \tag{5}$$

In this case b is the wing span. It is then possible to express the aerodynamic forces as a function of the degrees of freedom of the aeroelastic system, as in Eq. (6).

$$\boldsymbol{f}_a = \boldsymbol{C}^{DB}_{body}\left(\boldsymbol{T}_1\boldsymbol{x}_i' + \boldsymbol{T}_0\boldsymbol{x}_i\right) = \boldsymbol{D}^{DB}_1\boldsymbol{x}_i' + \boldsymbol{D}^{DB}_0\boldsymbol{x}_i \tag{6}$$

The equation Eq. (6) represents the first two elements of a series expansion of the aerodynamic forces in frequency domain

$$\boldsymbol{f}_a = \bar{\boldsymbol{D}}_0\boldsymbol{a} + \bar{\boldsymbol{D}}_1\boldsymbol{a}' + \bar{\boldsymbol{D}}_3\boldsymbol{a}'' + \ldots \tag{7}$$

The unsteady aerodynamic forces expressed by the state-space model in Eq. (2) already contains all the

unsteady terms of the series expansion and only the first two elements need to be corrected using the values from Eq. (6). The correction is implemented following the approach suggested in[18] and in[19], that is by substituting the 6×6 block of the matrices $\bar{\boldsymbol{D}}_0$ and $\bar{\boldsymbol{D}}_1$ associated with the body rigid motion with the matrices $\boldsymbol{D}_0^{DB}$ and $\boldsymbol{D}_1^{DB}$, and then discarding the aerodynamic coefficients predicted by the DLM. In order to implement the correction it is convenient to recast the state-space model in a form that contains explicitly the first two terms of the series expansion Eq. (7. This is obtained by using only the second derivative of the input for the forcing of the state equation, as shown in Eq. (8).

$$\begin{cases} \boldsymbol{x}_a' = \boldsymbol{A}\boldsymbol{x}_a + \bar{\boldsymbol{B}}_2 \boldsymbol{a}'' \\ \boldsymbol{f}_a/q_\infty = \boldsymbol{C}\boldsymbol{x}_a + \bar{\boldsymbol{D}}_0 \boldsymbol{a} + \bar{\boldsymbol{D}}_1 \boldsymbol{a}' + \boldsymbol{D}_2 \boldsymbol{a}'' \end{cases} \tag{8}$$

where $\bar{\boldsymbol{B}}_2 = \boldsymbol{A}^{-2}\boldsymbol{B}$, $\bar{\boldsymbol{D}}_0 = \boldsymbol{D}_0 - \boldsymbol{C}\boldsymbol{A}^{-1}\boldsymbol{B}$ and $\bar{\boldsymbol{D}}_1 = \boldsymbol{D}_1 - \boldsymbol{C}\boldsymbol{A}^{-2}\boldsymbol{B}$. This form allows to lump all the steady response to $\boldsymbol{a}$ and $\boldsymbol{a}''$ in the matrices $\bar{\boldsymbol{D}}_0$ and $\bar{\boldsymbol{D}}_1$, that can then be directly corrected using Eq. (6).

When unsteady aerodynamic forces are corrected using tabulated coefficients some care must also be devoted to the generalized forces due to gust input. The gust response is characterized by the time delay given by the gust penetration, but the effect of the delay vanishes at zero frequency, meaning that the penetration effect is absent in the steady response to a sustained gust. This means that in the limit of zero frequency the aerodynamic forces due to gust are equivalent to a change in angle of attack and sideslip of the aircraft and this equivalence must be preserved also when tabulated coefficients are used to correct aerodynamic forces. The same correction procedure used for the rigid body motion described above can be applied to the correction of the gust input, provided that an equivalent of Eq. (6) is obtained for gust input.

$$\boldsymbol{f}_{ag} = \boldsymbol{D}_{0g}^{DB} \frac{1}{V_\infty} \begin{bmatrix} U_y \\ U_z \end{bmatrix} = \begin{bmatrix} -\boldsymbol{C}_{body}^{\beta} & \boldsymbol{C}_{body}^{\alpha} \end{bmatrix} \frac{1}{V_\infty} \begin{bmatrix} U_y \\ U_z \end{bmatrix} \tag{9}$$

where U_y and U_z are the lateral and vertical components of the gust velocity, and $\boldsymbol{C}_{body}^{\beta}$ and $\boldsymbol{C}_{body}^{\alpha}$ are the columns of $\boldsymbol{C}_{body}^{DB}$ associated with the sideslip angle and angle of attack. In Eq. (9) only the correction for $\bar{\boldsymbol{D}}_0$ is defined, this means that for the gust input no correction is introduced in $\bar{\boldsymbol{D}}_1$.

4. MODE ACCELERATION METHOD

The dynamic response of the aircraft is simulated using a reduced basis for the definition of the structural deformation, composed by a series of natural modes augmented with additional shapes representing the rigid motion of the aircraft, the deflection of control surfaces and static deformation shapes. If the discretized FEM equations of motion of the aircraft are written as

$$\boldsymbol{M}\ddot{\boldsymbol{y}} + \boldsymbol{K}\boldsymbol{y} = \boldsymbol{b}(t) \tag{10}$$

where $\boldsymbol{b}$ is the input vector, representing the forces developed by aerodynamics, rotors and actuators. This input vector could be seen as composed by $\boldsymbol{b}(t) = \boldsymbol{B}_0 \boldsymbol{\beta}(t)$ a spatial distribution plus a term function of time. Internal forces in the structure can be obtained directly from the deformation of the model using the linear elastic constitutive law, so

$$\boldsymbol{L}(t) = \boldsymbol{S}_{load} \boldsymbol{y}(t) \tag{11}$$

The matrix $\boldsymbol{S}_{load}$ can be defined based on the structural finite element model (it can be extracted from NASTRAN using the Monitor Point 3 formulation[6]).

The basic idea of the modal truncation method is to compute the eigensolutions, and select a limited number of modes N to be used as degrees of freedom, so that the response of the system through can be written as

$$\boldsymbol{y} = \sum_{i=1}^{N} \boldsymbol{\phi}_i q_i = \boldsymbol{\Phi}\boldsymbol{q}. \tag{12}$$

Using unit mass normalization of modal coordinates, eq.(10) becomes

$$\ddot{\boldsymbol{q}} + \boldsymbol{\Omega}^2 \boldsymbol{q} = \boldsymbol{\Phi}^T \boldsymbol{b} \tag{13}$$

where

$$\boldsymbol{\Omega}^2 = \mathrm{Diag}[\omega_i^2] \tag{14}$$

is the diagonal matrix of the square of the mode frequencies.

Internal forces in the structure can be obtained directly from the deformation of the model as expressed by the superposition of reduced basis modes, i.e.

$$\boldsymbol{L}(t) = \boldsymbol{S}_{load} \boldsymbol{\Phi} \boldsymbol{q}(t). \tag{15}$$

This approach, called *direct recovery*[10], requires the use of a large number of normal modes and static shapes in order to get an accurate reconstruction of loads, since all the deformation shapes that are contributing to the selected load quantity need to be included in the basis, even if their dynamics is very fast and it is not excited during the response[9,6]. This difference is due to the fact that the mode shapes are not selected taking care of the spatial distribution of loads represented by the matrix $\boldsymbol{B}_0$.

A different approach can be used to improve the convergence of the reduced basis in the recovery of loads, which consist in considering both the static response of the complete structure and the dynamic response associated with the reduced basis. This method, called *mode acceleration*[10,9,20], gives a better convergence of the internal loads with respect to the number of modes used since it requires only the modes whose dynamics is actually excited by the external forces.

Reconsidering eq.(10) it is possible to write, and taking into account that modes not retained will not show any significant dynamics

$$\boldsymbol{K}\boldsymbol{y} = \boldsymbol{B}_0\boldsymbol{\beta}(t) - \boldsymbol{M}\boldsymbol{\Phi}\ddot{\boldsymbol{q}}, \tag{16}$$

and so the internal loads will be

$$\boldsymbol{L}(t) = \boldsymbol{S}_{load}\boldsymbol{K}^{-1}\left(\boldsymbol{B}_0\boldsymbol{\beta}(t) - \boldsymbol{M}\boldsymbol{\Phi}\ddot{\boldsymbol{q}}\right). \tag{17}$$

Unfortunately for an aeroelastic model, the external aerodynamic loads are function of the modal coordinates too, as shown by eq.(2). So, ideally, it is necessary to recover the matrices that project the unsteady aerodynamic forces computed by eq.(2) back onto the the nodes of the model. However, those matrices are not available in a time domain formulation, but only in frequency domain. On the other hand, there is no necessity of a time-domain representation of the matrices $\boldsymbol{H}^*_{am}(j\omega)$ and $\boldsymbol{H}^*_{ag}(j\omega)$, that provide the structural forces associated with modal structural displacements $\boldsymbol{q}$ and gust input α_g, since the internal loads are computed in a post-processing step after the dynamic simulation, and the the computation of the aerodynamic contribution to internal forces can be computed in frequency domain and then transformed in time domain using an inverse Fourier transformation.

The contribution to internal loads from aerodynamic forces is then computed by transforming in frequency domain the time histories of the modal displacements $\boldsymbol{q}(t)$ and of the gust input $\alpha_g(t)$, computing the aerodynamic loads in frequency domain and transforming back the loads in time domain. The numerical implementation of the procedure requires the use of a discrete Fourier transform and then requires a stable time response in order to be consistent with the implicit periodicization of the signal. The requirement of stable response is not an issue since load computations are usually performed on stable systems, but can lead to some problems associated with the rigid motion of the aircraft due to the fact that there is no restraining force that operates on the absolute position of the aircraft in space. Aerodynamic forces are associated with the relative motion of the aircraft with respect to the airflow, and not with the absolute position of the aircraft itself. This is reflected by the presence of a series of zeroes in the state-space model of the aeroelastic aircraft, showing that there is no change in the model properties with a change of the position in space[21]. The numerical computation of aerodynamic forces, however, can lead to systems where the system poles associated with the aircraft absolute position are slightly unstable instead of being perfect integrators. In addition the absolute position of the aircraft can have a small, nonphysical contribution to structural loads in Eq. (20). This means that the reconstructed loads can present some oscillations due both to the slightly unstable modes and by the absolute position of the aircraft affecting the internal loads. In order to avoid this problem it is possible to convert the rigid motion of the aircraft from inertial to body axes[19]. Body axes coordinates are directly related to the motion of the aircraft with respect to the airflow and are then less sensitive to numerical errors. The transformation consists in transforming the absolute motion of the aircraft $\boldsymbol{r}^I(j\omega)$ to the velocity components in body frame $\boldsymbol{v}^B(j\omega) = [u, v, w]^T$. In the same way the orientation of the aircraft $\boldsymbol{\theta}^I(j\omega)$ is transformed in the components of the rotational velocity in body axes $\boldsymbol{\omega}^B(j\omega) = [p, q, r]^T$. The transformation is frequency-dependent since it implies the derivation of displacements and rotations to get velocities and rotational velocities and it is represented by Eq. (18)[17]

$$\begin{aligned}\begin{bmatrix}\boldsymbol{v}^B(j\omega)\\ \boldsymbol{\omega}^B(j\omega)\end{bmatrix} &= \begin{bmatrix}j\omega\boldsymbol{I} & \boldsymbol{v}_0\times\\ \boldsymbol{0} & j\omega\boldsymbol{I}\end{bmatrix}\begin{bmatrix}\boldsymbol{r}^I(j\omega)\\ \boldsymbol{\theta}^I(j\omega)\end{bmatrix}\\ &= \boldsymbol{T}(j\omega)\begin{bmatrix}\boldsymbol{r}^I(j\omega)\\ \boldsymbol{\theta}^I(j\omega)\end{bmatrix}\end{aligned} \tag{18}$$

where $\boldsymbol{v}_0$ is the vector defining the flight velocity of the aircraft. The inverse of this transformation can be used to transform aerodynamic unsteady forces related to the rigid motion from the inertial to the body-axes coordinates, providing that the dimensional frequency is transformed to the reduced frequency $k = \omega l_a / V_\infty$

$$\begin{aligned}&\begin{bmatrix}\boldsymbol{H}^v(jk) & \boldsymbol{H}^\omega(jk)\end{bmatrix}\\ &= \begin{bmatrix}\boldsymbol{H}^r(jk) & \boldsymbol{H}^\theta(jk)\end{bmatrix}\boldsymbol{T}^{-1}(jk)\end{aligned} \tag{19}$$

the transformation above transforms the aerodynamic forces associated with the inertial displacements and rotations, respectively $\boldsymbol{H}^r$ and $\boldsymbol{H}^\theta$, in forces associated with the body velocity and rotational velocity (respectively $\boldsymbol{H}^v$ and $\boldsymbol{H}^\omega$).

Consequently, the recovering internal loads directly from the time histories of all the applied external forces, will be equal to

$$\boldsymbol{L} = \boldsymbol{S}_{load}\boldsymbol{K}^{-1}\left[\boldsymbol{f}^{rot} + \boldsymbol{f}^{act} + q_\infty \boldsymbol{f}^*_a - \boldsymbol{M}\boldsymbol{U}\ddot{\boldsymbol{q}}\right] \tag{20}$$

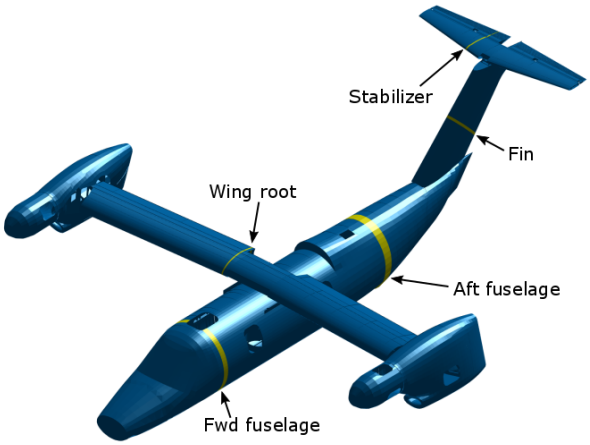

Figure 2: Monitoring stations.

where

(21)
$$\boldsymbol{f}_a^* = \mathcal{F}^{-1}\left(\boldsymbol{H}_{am}^*(j\omega)\mathcal{F}(\boldsymbol{q}(t)) + \boldsymbol{H}_{ag}^*(j\omega)\mathcal{F}(\boldsymbol{\alpha}_g)\right),$$

and in addition there are also the loads transmitted to the structure by the rotors and and actuators $\boldsymbol{f}^{rot}$ and $\boldsymbol{f}^{act}$.

5. RESULTS

The evaluation of the methods described in the preceding section consists in two main parts:

- A study of the convergence of gust loads with the model size using both the direct recovery method currently employed and the mode acceleration method. Both peak loads in deterministic gust responses and the variance of loads in stochastic turbulence analyses will be considered.
- A study of the sensitivity of the gust loads with respect to the modification of the aerodynamic matrices.

Internal forces on the AW609 airframe will be recovered considering the sections shown in Fig. 2.

5.1. Gust response

The mode acceleration method and the direct load recovery are compared firstly by considering the time response to a deterministic gust, defined according to aircraft certification regulations[22,23,24]. A vertical gust is considered here, with a length $H = 200$ ft with the tiltrotor in forward flight and at sea level. Three different sections are considered here for the evaluation of the loads among the ones presented in Fig. 2: the wing root station, the forward fuselage section and the stabilizer section. The time histories of the response are presented in Fig. 3 and Fig. 4, comparing the results obtained with the direct recovery and the mode acceleration method, obtained using 20 or 240 natural modes.

The wing root bending moment is well reconstructed using 20 modes and using both the mode acceleration and the direct recovery method, as shown in Fig. 3(a). This indicates that only the low frequency modes contribute significantly to the deformation associated with the bending moment at wing root, and their dynamics is completely captured using the a small basis. For the torsional moment at wing root, however, the convergence is slower and if the direct recovery method is used there is a sensible difference between the load obtained using 20 modes and the one obtained using 240 modes, as shown in Fig. 3(b). In this case the mode acceleration method is instead able to provide converged loads using 20 modes, meaning that all the modes participating dynamically to the response are contained in this reduced set.

The time history of the bending moment evaluated at the forward fuselage station is presented in Fig. 4(a), and presents convergence properties very similar to the wing root bending moment in Fig. 3(b), even if from the time history it is possible to see that higher frequency components are participating to the response. A completely different behaviour is obtained for the stabilizer, as shown in Fig. 4(b). In this case the direct recovery method provides very different results when 20 modes are used instead of 240, and still the value obtained using 240 modes is far from the value obtained with the mode acceleration method. The mode acceleration method is instead providing the same results regardless of the number of modes used, showing that also for this section all the dynamic response is captured using 20 modes.

The convergence of the two methods can be studied by considering the variation of the maximum predicted load with the variation of the modal basis used. The computation is performed using three different gust gradient lengths: 30 ft, which is the shortest gust prescribed by regulations, 350 ft, which is the longest one and 100 ft representing an intermediate value. The convergence of the wing root bending moment is presented in Fig. 6, and shows that for this particular load component the mode acceleration and the direct recovery methods possess very similar convergence properties, with the only major difference being the possibility of the mode acceleration method to estimate inter-

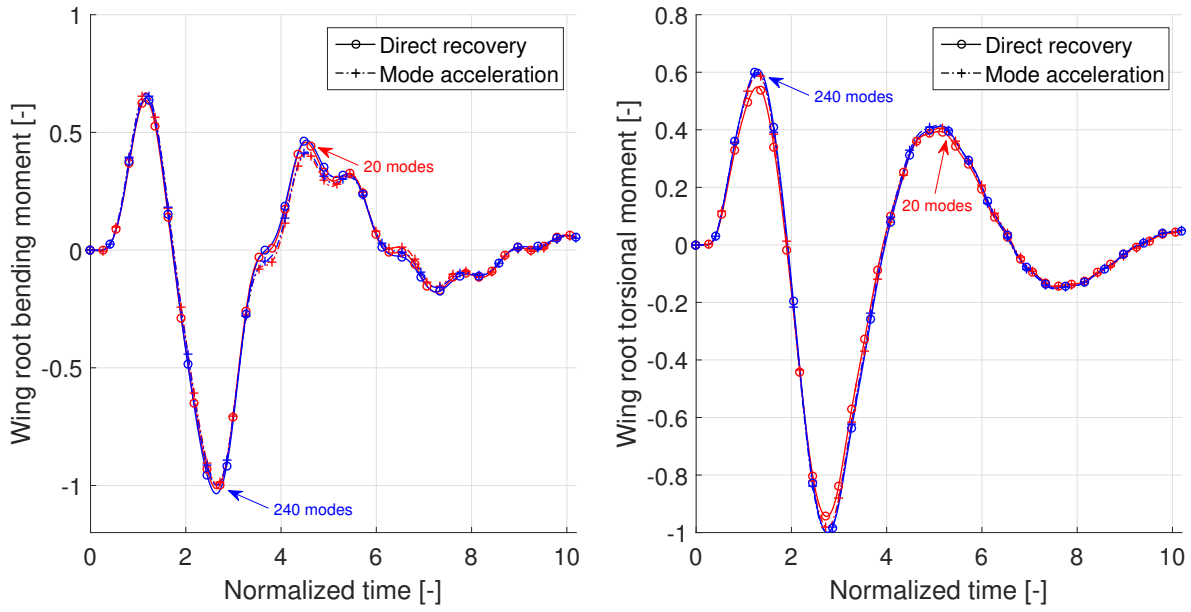

(a) Bending moment (b) Torsional moment

Figure 3: Time response to discrete gust at the wing root station.

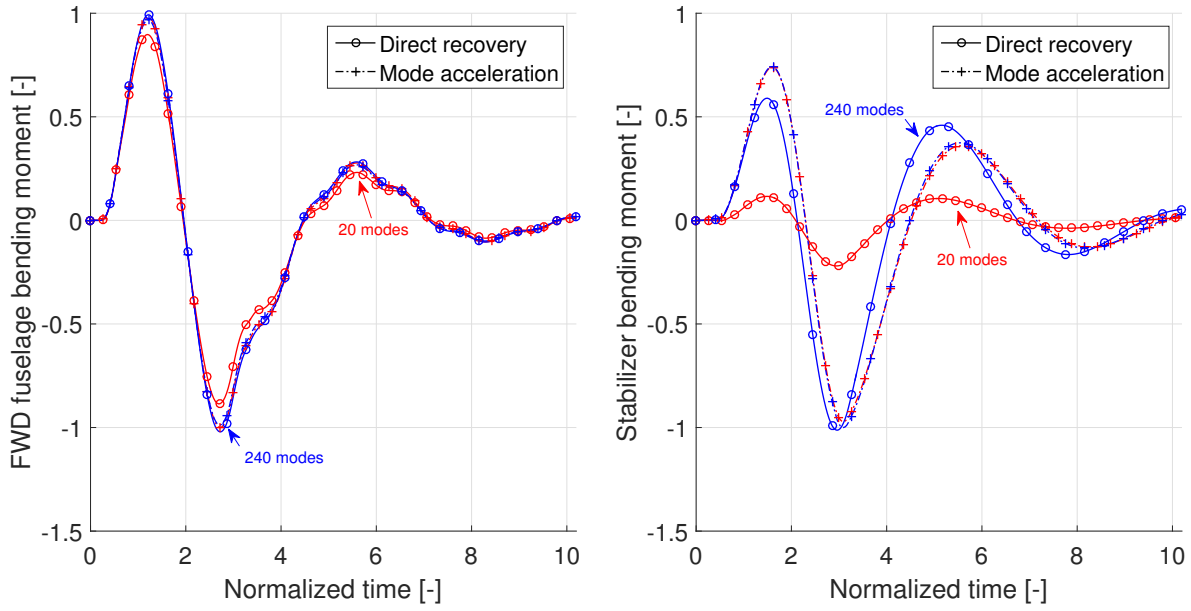

(a) FWD fuselage bending moment (b) Stabilizer bending moment

Figure 4: Time response to discrete gust.

nal forces also using only a rigid model. The very quick convergence of the maximum loads resulting from intermediate and slow gusts is in accordance with the results presented in the time histories of Fig. 3(a). The fast gust, instead, is able to excite higher frequency dynamics of the system and then requires a larger modal basis to get converged loads, regardless of the method used to recover them.

The convergence of the other load components is presented in Fig. 5, Fig. 7 and in Fig. 8. For all the stations considered it can be seen that the maximum loads provided by the mode acceleration method present less variation with the number of modes used, and in some cases also the value obtained with a rigid model is a good approximation of the converged value. This is the case for example for the stabilizer bending moment of Fig. 8 that for the intermediate and long gusts is dominated by the static response of the system and presents no sig-

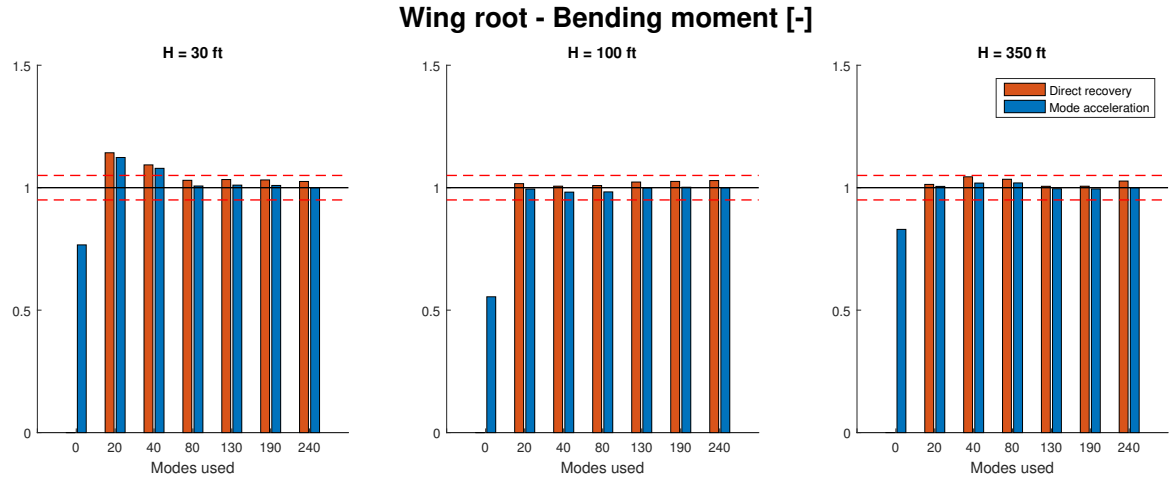

Figure 5: Convergence of wing root bending moment with the increase of modes used. Dashed lines represent the $+/-5\%$ difference with respect to the converged value.

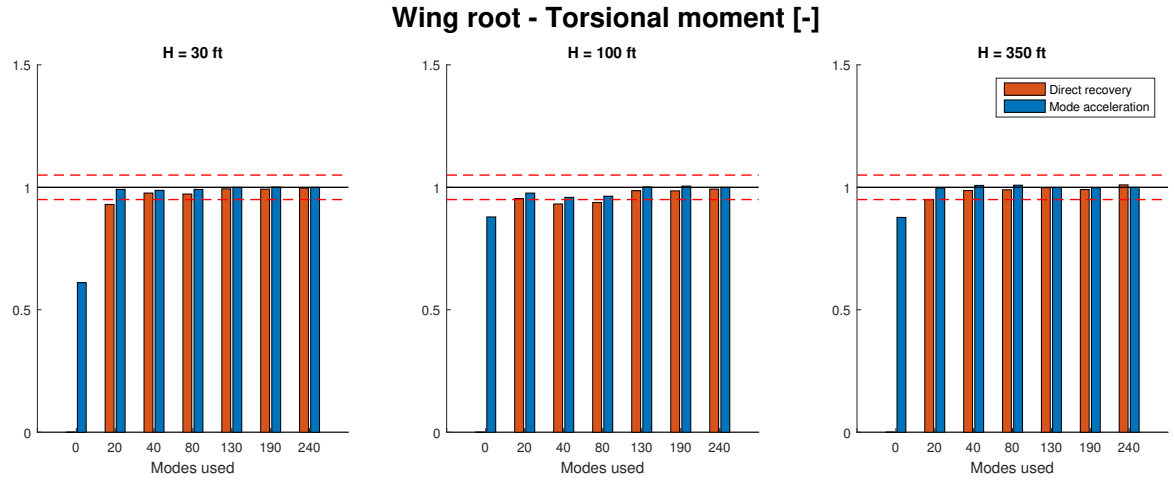

Figure 6: Convergence of wing root torsional moment with the increase of modes used. Dashed lines represent the $+/-5\%$ difference with respect to the converged value.

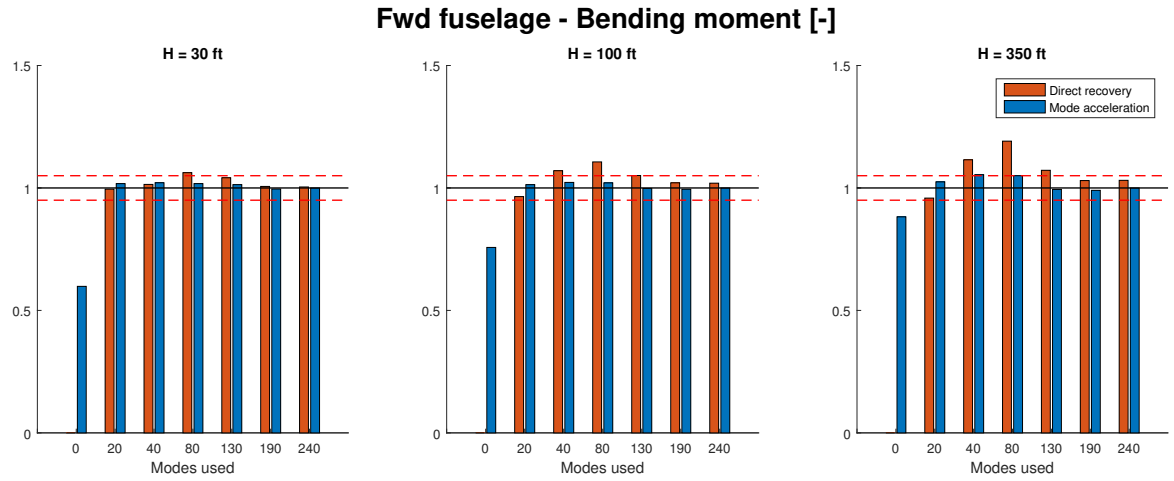

Figure 7: Convergence of forward fuselage bending moment with the increase of modes used. Dashed lines represent the $+/-5\%$ difference with respect to the converged value.

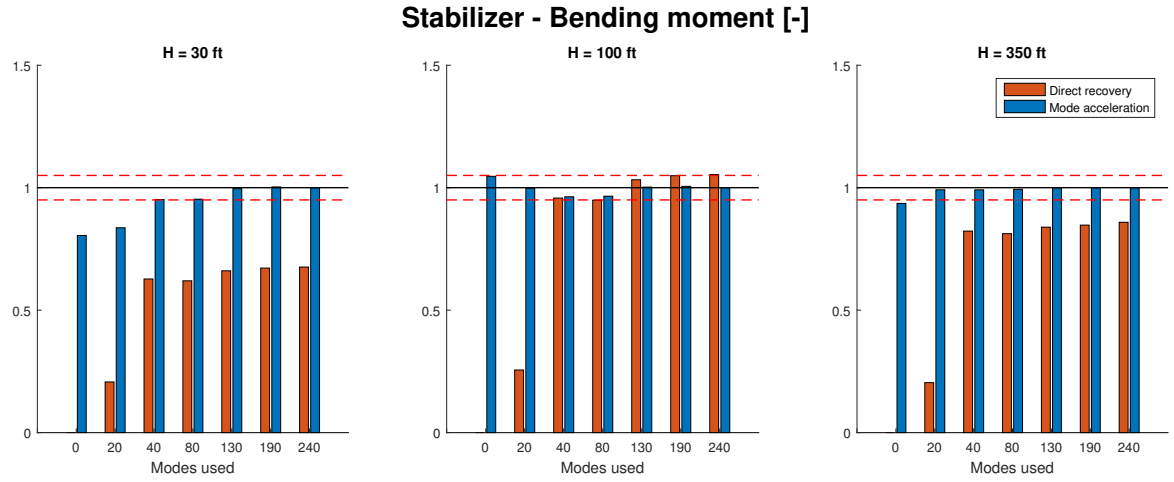

Figure 8: Convergence of stabilizer bending moment with the increase of modes used. Dashed lines represent the $+/-5\%$ difference with respect to the converged value.

nificant variation increasing the number of modes included in the basis.

5.2. Turbulence response

In addition to the discrete gust response, also the response to continuous turbulence is analyzed here, comparing the Power Spectral Density (PSD) functions of the loads obtained using the direct recovery and the mode acceleration methods. A Von Karman spectrum is used to excite the system, with bandwidth and amplitude described by certification regulations[22,23,24], the power spectral density of the load components is then extracted using a frequency-domain analysis.

As done for the time response to discrete gust, also for the continuous turbulence response the PSD obtained using 20 structural modes and 240 structural modes is compared in Fig. 9 for the wing root station. The response to continuous turbulence of the wing root bending moment is presented in Fig. 9(a). It is possible to see that only two modes are contributing significantly to the wing root bending moment, which are the short period and the symmetric wing bending mode. The amplitude of the response of the bending mode does not depend on the method used for load recovery, meaning that the dynamic response of that mode is well captured, while at lower frequencies the difference between the PSDs predicted by the two methods is larger, due to the different contribution of the static response of higher frequency modes. Also the torsional moment at wing root, presented in Fig. 9(b), is dominated by the response of two modes, the short period and the torsional mode and the peak of the response are well captured with both recovery methods.

The good agreement between the direct recovery and the mode acceleration methods in the determination of the PSD of the load components is also confirmed by the convergence of the Root Mean Square (RMS) of the loads with the increase in mode number shown in Fig. 10. The RMS is almost at convergence even when a small number of modes is used, both with the direct recovery and the mode acceleration methods.

The convergence of loads in the forward fuselage and the stabilizer sections is slower with respect to the convergence of internal forces at wing root. The bending moments in these two sections are dominated by the response of the short period mode, as seen in Fig. 11(a) and in Fig. 11(b). The short period mode is not associated with structural deformations and internal forces associated with its dynamic response can be included only if the static response of other flexible modes are accounted for, in order to allow the reconstruction of the deformation associated with the considered internal force. It can be seen in Fig. 11(b) that there is almost no dynamic contribution from deformable modes to the bending moment on the stabilizer section, and the internal force is obtained from the static response to the excitation of the short period. For this reason the convergence of this load component with the mode number is very slow, as seen in Fig. 12(b).

5.3. Gust response with aerodynamic coefficient correction

The effect of the inclusion of the aerodynamic coefficients on the recovered loads can be evaluated by considering the time response to a discrete gust. A significant portion of the time response is dominated by the rigid motion of the aircraft which in

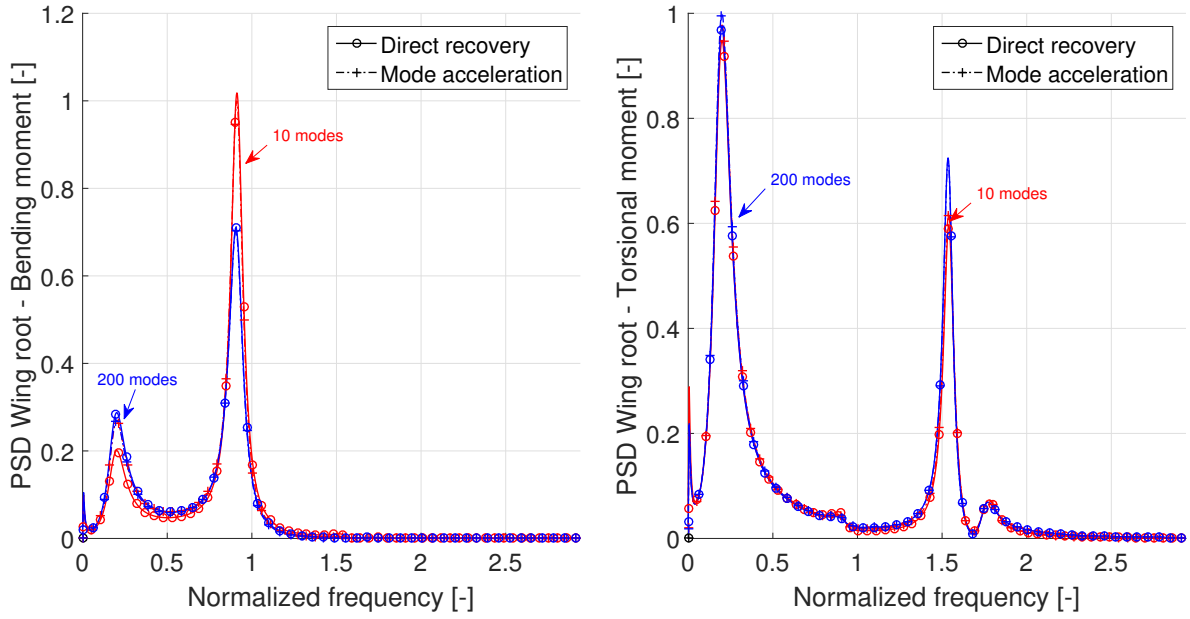

(a) Bending moment (b) Torsional moment

Figure 9: Power spectral density of the response to continuous turbulence defined with the Von Karman spectrum for the wing root section.

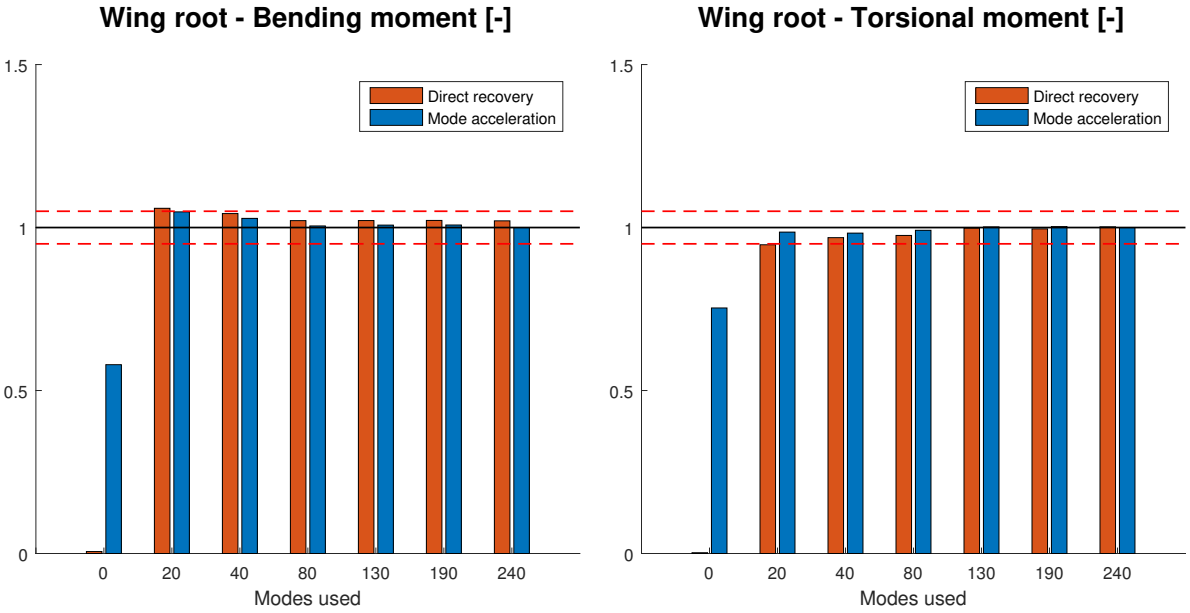

(a) Bending moment (b) Torsional moment

Figure 10: Convergence of the RMS of internal loads at wing root with the increase of modes used

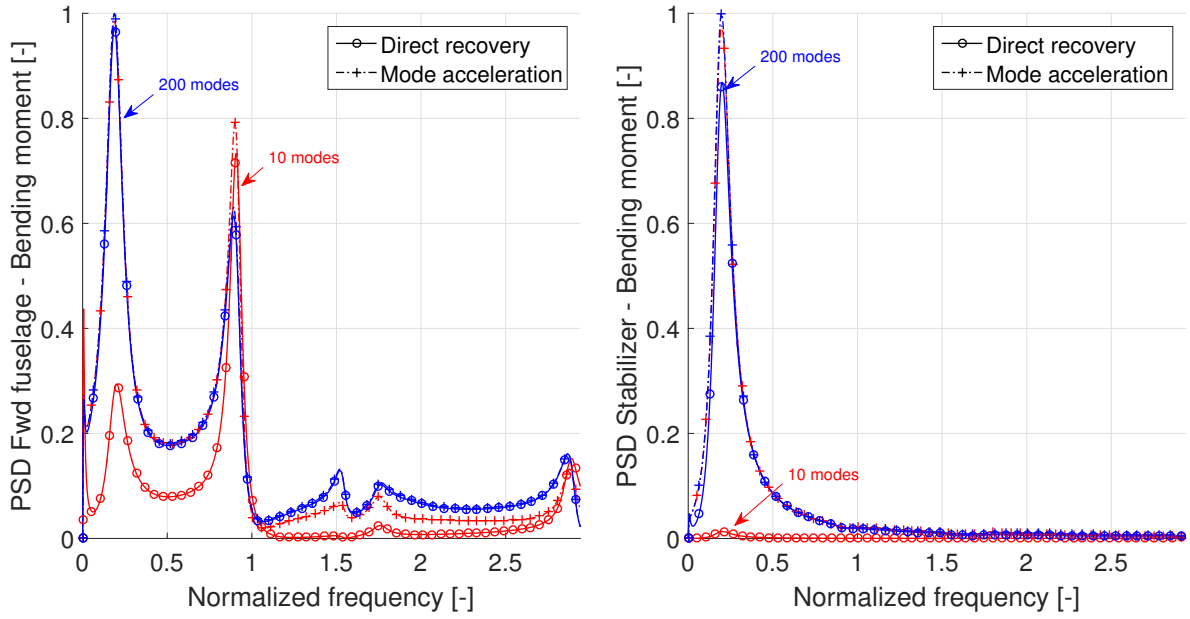

(a) FWD fuselage bending moment (b) Stabilizer bending moment

Figure 11: Power spectral density of the response to continuous turbulence defined with the Von Karman spectrum.

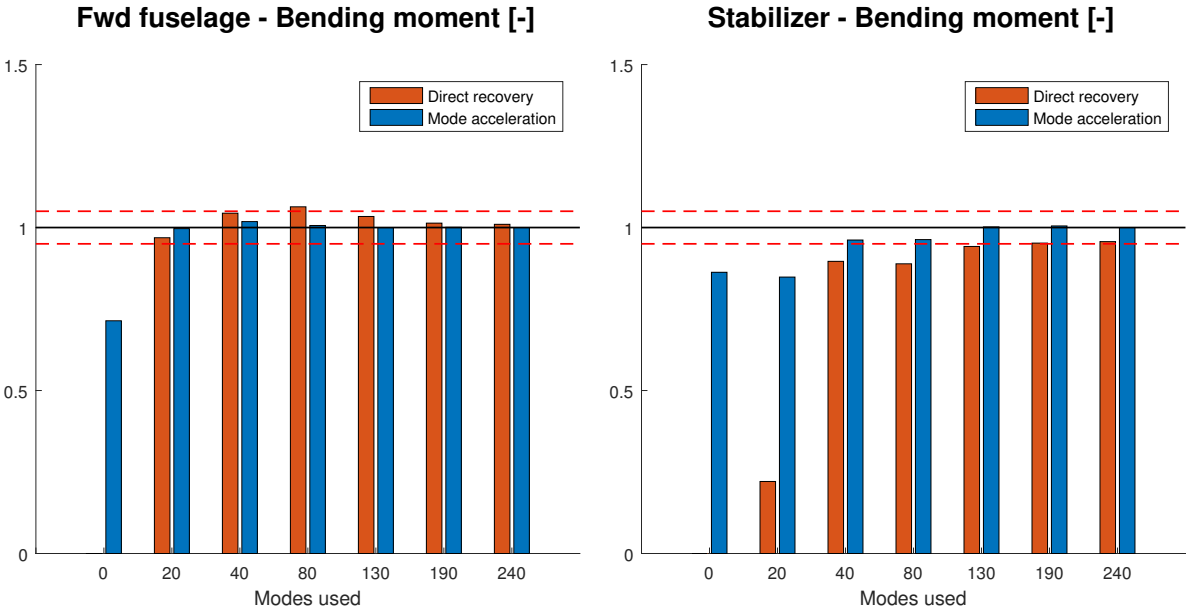

(a) FWD fuselage bending moment (b) Stabilizer bending moment

Figure 12: Convergence of the RMS of internal loads with the increase of modes used

turn is defined by the frequency and damping of the short period mode, if a vertical gust is considered. The time histories of the wing root bending and torsional moments are presented in Fig. 13(a) and in Fig. 13(a) respectively. It can be seen that when the aerodynamic forces are taken directly from the unsteady panel method (*Uncorrected* curve) the short period is lightly damped and the maximum load is associated with the second (negative) peak of the response. The introduction of aerodynamic coefficients allow to introduce in the model dynamics also effects that are not captured by the linear potential aerodynamic method, such as the interference of the nacelle and fuselage on the wing. In this way the dynamics of the rigid motion of the aircraft can be corrected, influencing the predicted loads, as seen in Fig. 13.

6. CONCLUSIONS

The presents work discussed two improvements that were introduced in the procedure used at Leonardo Helicopters to predict dynamic gust and turbulence loads on tiltrotors. The procedure is based on the coupling of a dynamic structural model of the airframe coupled with the rotor aeroelastic model, the actuator dynamics and the flight control system. The first improvement consisted in the introduction of the mode acceleration method for the recovery of loads, that allows the use of a very small reduced basis for the evaluation of dynamic loads, ensuring an excellent accuracy while allowing very efficient simulation. The second improvement consisted in the development of a methodology for the correction of the unsteady aerodynamic forces using tabulated aerodynamic coefficients. This correction is very useful for an aircraft with a complex aerodynamic configuration as a tiltrotor since it allows to predict correctly the overall dynamics of the rigid body motion, which has direct influence on the predicted loads.

REFERENCES

[1] TM Gaffey, JG Yen, and RG Kvaternik. Analysis and model tests of the proprotor dynamics of a tilt-proprotor vtol aircraft. In *Air Force V/STOL Technology and Planning Conference*, pages 23–25, 1969.

[2] Wayne Johnson. Optimal control alleviation of tilting proprotor gust response. *Journal of Aircraft*, 14(3):301–308, 1977.

[3] Tom Parham Jr and Lawrence M Corso. Aeroelastic and aeroservoelastic stability of the BA 609. In *25th European Rotorcraft Forum*, Rome, Italy, 1999.

[4] Pierangelo Masarati, Vincenzo Muscarello, and Giuseppe Quaranta. Linearized aeroservoelastic analysis of rotary-wing aircraft. In *36th European Rotorcraft Forum*, pages 099.1–10, Paris, France, September 7–9 2010.

[5] Pierangelo Masarati, Vincenzo Muscarello, Giuseppe Quaranta, Alessandro Locatelli, Daniele Mangone, Luca Riviello, and Luca Viganò. An integrated environment for helicopter aeroservoelastic analysis: the ground resonance case. In *37th European Rotorcraft Forum*, pages 177.1–12, Gallarate, Italy, September 13–15 2011.

[6] A. Rigo, M. Favale, A.A. Trezzini, and G. Quaranta. Numerical evaluation of gust loads on tiltrotor. In *74th AHS Forum, Phoenix*, 2018.

[7] Vincenzo Muscarello, Francesca Colombo, Giuseppe Quaranta, and Pierangelo Masarati. Aeroelastic rotorcraft–pilot couplings in tiltrotor aircraft. *Journal of Guidance, Control, and Dynamics*, 42(3):524–537, 2018.

[8] Alberto Rigo, Vincenzo Muscarello, Pierangelo Masarati, Giuseppe Quaranta, and Marco Favale. Drive train modeling effects on tiltrotor aeroelastic analysis. In *AIAA Scitech 2019 Forum*, 2019.

[9] JM Dickens, JM Nakagawa, and MJ Wittbrodt. A critique of mode acceleration and modal truncation augmentation methods for modal response analysis. *Computers & Structures*, 62(6):985–998, 1997.

[10] Raymond L Bisplinghoff, Holt Ashley, and Robert L Halfman. *Aeroelasticity*. Dover Publications, INC. Mineola, New York, 1996.

[11] William P Rodden and Erwin H Johnson. *MSC/NASTRAN aeroelastic analysis: User's guide; Version 68*. MacNeal-Schwendler Corporation, 1994.

[12] Wayne Johnson. Technology drivers in the development of camrad ii. In *American helicopter society aeromechanics specialists conference, San Francisco, California*, 1994.

[13] E Albano and W P Rodden. A Doublet–Lattice Method for Calculating the Lift Distributions on Oscillating Surfaces in Subsonic Flow. *AIAA Journal*, 7(2):279–285, 1969.

[14] K L Roger. Airplane Math Modeling Methods for Active Control Design. Technical Report CP–228, AGARD, 1977.

[15] Giovanni Pasinetti and Paolo Mantegazza. Single Finite States Modeling of Aerodynamic Forces Related to Structural Motions and Gusts. *AIAA Journal*, 37(5):604–612, 1999.

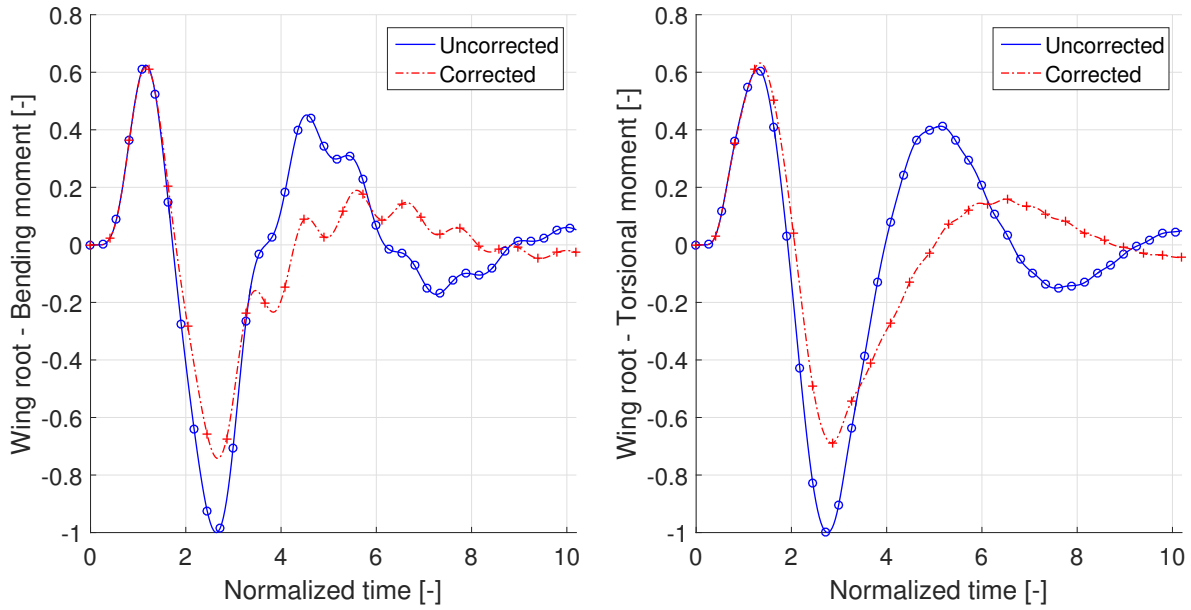

(a) Wing root bending moment

(b) Wing root torsional moment

Figure 13: Effect of aerodynamic coefficient correction on the gust response

[16] Moti Karpel, Boris Moulin, and PC Chen. Dynamic response of aeroservoelastic systems to gust excitation. *Journal of Aircraft*, 42(5):1264–1272, 2005.

[17] Kajal K Gupta, MJ Brenner, and LS Voelker. Development of an integrated aeroservoelastic analysis program and correlation with test data. Technical report, NASA-TP-3120, 1991.

[18] Dario Baldelli, P. Chen, Jose Panza, and Joshua Adams. Unified rational function approximation formulation for aeroelastic and flight dynamics analyses. In *Structures, Structural Dynamics, and Materials and Co-located Conferences*. American Institute of Aeronautics and Astronautics, May 2006. 0.

[19] Federico Fonte and Sergio Ricci. Recent developments of neocass the open source suite for structural sizing and aeroelastic analysis. In *International Forum on Aeroelasticity and Structural Dynamics*, 2019. IFASD-2019-021.

[20] Paolo Mantegazza. Tutorial on attached-mean axes and their use in the calculation of deformable static and damped-undamped vibration modes of a free-free structure. *Journal of Aeroelasticity and Structural Dynamics*, 2(1), 2011.

[21] Federico Fonte. *Design and validation of active gust load alleviation systems for aircraft*. PhD thesis, Politecnico di Milano, Milano (Italy), 2018.

[22] F.M. Hoblit. *Gust Loads on Aircraft: Concepts and Applications*. AIAA education series. American Institute of Aeronautics & Astronautics, 1988.

[23] Anon. *Federal Regulation Part 25 - Airworthiness Standards: Transport Category Airplanes*. Federal Aviation Administration, 2017.

[24] Anon. *Certification Specifications for Large Aeroplanes CS-25*. European Aviation Safety Agency, 2009. Amendment 7, Annex to ED Decision 2009/013/R.